Enhanced Dissolution of Manganese Oxide in Ice Compared to Aqueous Phase under Illuminated and Dark Conditions

Kitae Kim,[†] Ho-Il Yoon,[‡] and Wonyong Choi*,[†]

[†]School of Environmental Science and Engineering, Pohang University of Science and Technology (POSTECH), Pohang 790-784, South Korea

[‡]Korea Polar Research Institute, Incheon 406-840, South Korea

ABSTRACT: Manganese is one of the common elements in the Earth's crust and an essential micronutrient for all living things. The reductive dissolution of particulate manganese oxide is a dominant process to enhance mobility and bioavailability of manganese for the use of living organisms. In this work, we investigated the reductive dissolution of manganese oxides trapped in ice (at -20 °C) under dark and light irradiation (visible: $\lambda > 400$ nm and UV: $\lambda > 300$ nm) in comparison with their counterparts in aqueous solution (at 25 °C). The reductive dissolution of synthetic MnO_2, which took place slowly in aqueous solution, was significantly accelerated in ice phase both in the presence and absence of light: about 5

times more dissolution in ice phase than in liquid water after 6 h UV irradiation in the presence of formic acid. The enhanced dissolution in ice was observed under both UV and visible irradiation although the rate was much slower in the latter condition. The reductive dissolution rate of $Mn(II)_{aq}$ (under both irradiation and dark conditions) gradually increased with decreasing pH below 6 in both aqueous and ice phases, and the dissolution rates were consistently faster in ice under all tested conditions. The enhanced generation of $Mn(II)_{aq}$ in ice can be mainly explained in terms of freeze concentration of electron donors, protons, and MnO_2 in liquid-like ice grain boundaries. The outdoor solar experiment conducted in Arctic region (Ny-Ålesund, Svalbard, 78°55′N) also showed that the photoreductive dissolution of manganese oxide is enhanced in ice. The present results imply that the dissolution of natural minerals like manganese oxides can be enhanced in icy environments such as polar region, upper atmosphere, and frozen soil.
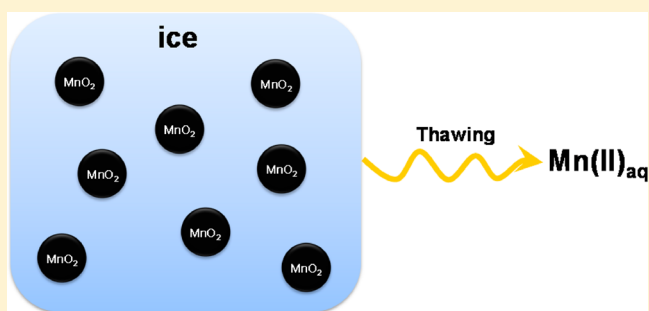
INTRODUCTION

The redox transformation of micronutrients (e.g., iron and manganese) plays the critical role in the environmental biogeochemistry since the redox speciation controls the mobility, bioavailability, and environmental fate of the mineral elements.[1] Manganese is one of the abundant elements in earth's crust and an essential micronutrient, like iron, for all organisms and is involved in important redox transformations in the environment. Manganese oxides can readily oxidize As(III) to As(V), Cr(III) to Cr(VI), Co(II) to Co(III), Se(IV) to Se(VI), and organic compounds.[2,3] Solid oxides of Mn(III) or Mn(IV) are thermodynamically favored than soluble Mn(II) in oxygenated natural environment. The transformation of solid manganese oxide (Mn^{III}, Mn^{IV}) to soluble manganese (Mn^{II}) is very important since the particulate form of MnO_2 is not directly available for living organisms. Manganese oxide can be reduced by organic compounds and natural organic matters,[4−8] which influences manganese cycling in the environment and the bioavailability of manganese to plants and microorganisms. For example, it was demonstrated that manganese dioxide in seawater can be photoreduced to Mn^{2+} in the presence of marine humic acid,[4,7,9] which can be similarly compared with the photoreductive dissolution of iron oxides.[10]

Aquatic chemical reactions are generally slowed down with decreasing temperature. However, unexpectedly fast reactions have been observed in ice phase above the eutectic point.[11−14] The freeze-concentration effect (referring to exclusion and subsequent concentration of organic and inorganic solutes from ice crystals into liquid-like ice grain boundaries upon freezing) is regarded as a main driving force for the accelerated reactions in ice phase.[11−21] The oxidation of nitrite (NO_2^-) to nitrate (NO_3^-) in oxic environment, which is very slow in aqueous phase, is extremely accelerated by freezing up to a factor of 10^5, which was ascribed to the freeze concentration of NO_2^-, proton, and oxygen confined in unfrozen solution between ice crystals.[11,12] Photochemical processes taking place in snow and ice can be also markedly different from those in aqueous solution when the light-absorbing substrates are highly concentrated within the grain boundaries.[22,23] Such photochemical reaction in snow and ice can significantly alter the atmospheric composition near snow/ice covered boundary
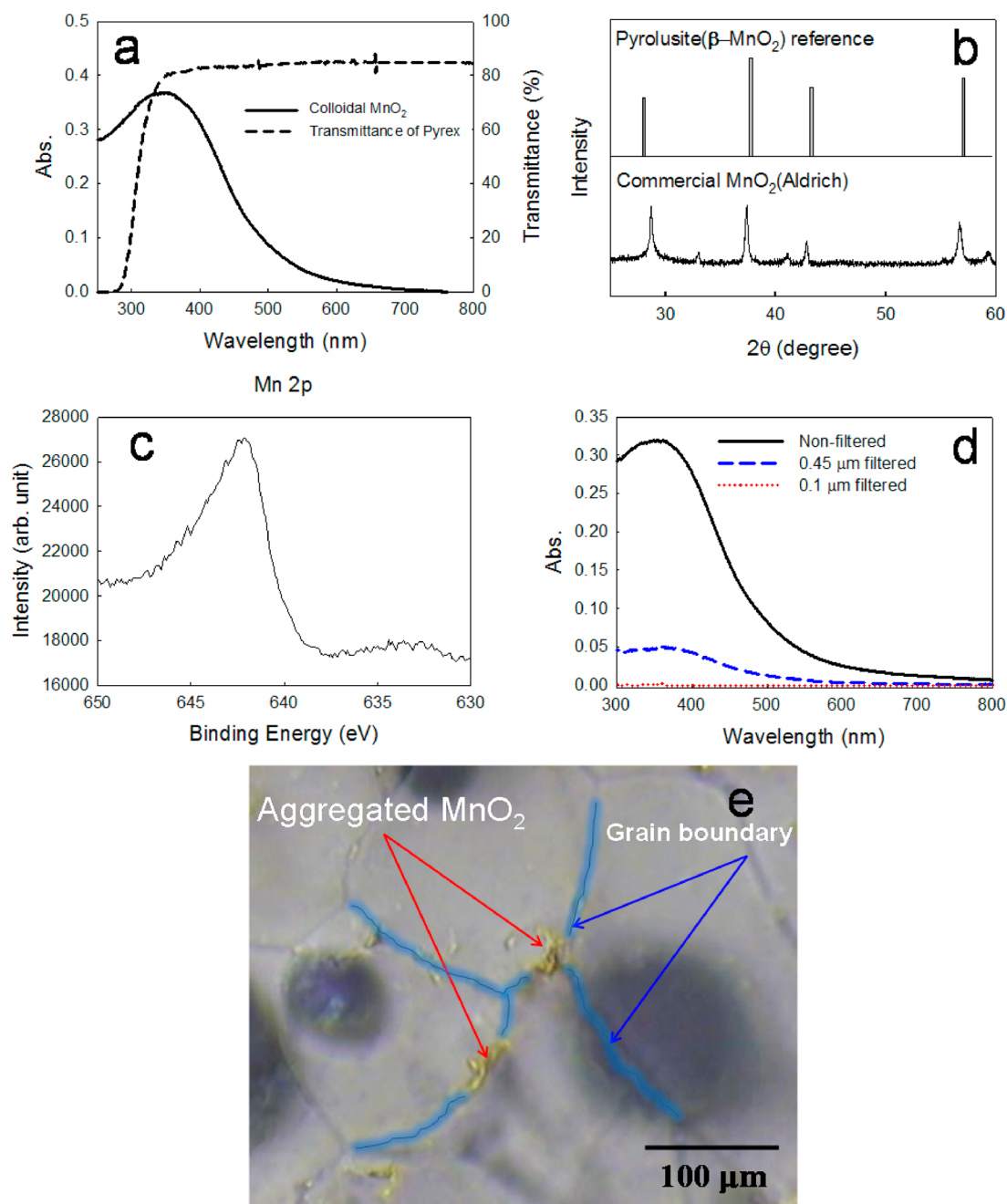
Figure 1. (a) UV−visible absorption spectrum of MnO_2 colloid and the transmittance of pyrex filter. (b) XRD pattern of reference birnessite and the synthesis MnO_2. (c) XPS spectrum for the Mn 2p band of colloidal MnO_2 (d) Change of UV−visible absorption spectrum of colloidal MnO_2 after filtration with different pore-size filters. (e) Optical image of ice with highly aggregated MnO_2 particles in ice grain boundary region at −20 °C.

regions by releasing nitrogen oxide, nitrous acid, light aldehydes, acetone, and molecular halogens, which are generated from the reactions of hydroxyl radicals (produced by nitrate photolysis) with natural organic matters and halide ions.[24] The photochemical transformation of organic pollutants in ice phase might generate products different from those in the aqueous phase and influence the fate of chemical pollutants in icy environment.[22,23,25] Our research group recently reported that the production of bioavailable iron $(Fe(II)_{aq})$ via photoreductive dissolution of iron oxide particles is markedly enhanced in ice phase compared to that in aqueous phase.[13] We also found that the reduction of hexavalent $Cr(VI)$ by organic acids is significantly accelerated in ice phase.[14] Although the importance of environmental chemical processes occurring in

ice is being recognized, studies on the chemical reactions in ice are very few and particularly the heterogeneous environmental processes remain unexplored.

In this study, we focus our attention on the reductive dissolution of manganese oxides (a component of mineral dusts, ambient aerosols, and soil) trapped in ice under both dark and light irradiation (visible and UV) in comparison with its aqueous counterparts. The dissolution processes between ice and aqueous phases are significantly different and the experimental parameters affecting the process, mechanism, and the environmental implications are discussed. The present study extends the specific case[13] of photochemical dissolution of iron oxides in ice to other mineral oxides in ice (regardless of

the presence of light), which more generalizes the effects of ice-enhanced dissolution of mineral oxides in the environments.

■ EXPERIMENTAL SECTION

Materials. All chemicals were of analytical-reagent grade and solutions were prepared with doubly distilled water. The colloidal manganese oxide was prepared by following a literature method.[26] To prepare the colloid, 10 mL of $KMnO_4$ (0.1 M) and 20 mL of $Na_2S_2O_3$ (18.8 mM) aqueous solutions were mixed together in a 2-L volumetric flask, and water was added to fill the volume and stirred. The colloidal MnO_2 was formed through the following stoichiometric reaction.

$$8MnO_4^- + 3S_2O_3^{2-} + 2H^+ = 8MnO_2(s) + 6SO_4^{2-} + H_2O$$
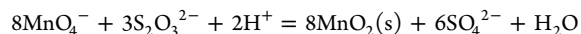
A dark-brown colloidal solution was obtained, which remained clear without coagulation at least for several months. The as-prepared colloidal MnO_2 (43.5 mg·MnO_2/L) was diluted to 4.35 mg/L in most experiments.

The absorption spectrum of colloidal MnO_2 was recorded with a UV−visible spectrophotometer (UV-2401PC Shimadzu), and showed a large visible absorption with a wide maximum around 300−400 nm (Figure 1a). The crystal phase of synthesized MnO_2 was confirmed by X-ray diffraction analysis (PANalytical X'Pert diffractometer with an X'Celerator detector) using Cu K_α radiation (Figure 1b). X-ray photoelectron spectroscopy was used to analyze the oxidation state of Mn in colloidal MnO_2 since the proportion of Mn(IV), Mn(III), and Mn(II) in synthesized colloidal MnO_2 is critical.[27] The Mn 2p spectrum of colloidal MnO_2 (Figure 1c) suggests that most of Mn in synthesized colloidal MnO_2 is present as a form of Mn(IV).

Dissolution Experiments in Ice. Aqueous colloidal solutions of manganese oxides (10 mL) were placed in 12 × 125-mm quartz tubes, added with appropriate electron donors, sealed with septa, and solidified in an ethanol bath cooled at −20 °C. The temperature of the freezing bath was gradually lowered from −5 to −20 °C within 30 min to prevent the breakage of the tubes. After freezing, the color of the ice containing colloidal manganese oxide was uniform along the ice column, which confirmed that MnO_2 particles were well dispersed without settling at the bottom. As for the photochemical dissolution experiments, sample tubes (maximum 16 tubes) were located in a merry-go-round photolysis reactor that was rotated at a constant speed (0.8−1.0 rpm) around a 100-W mercury lamp (Ace Glass Inc.) for uniform irradiation. The whole photolysis reactor was immersed along with the lamp in the ethanol bath. Light was filtered by a pyrex jacket (transmitting $\lambda > 300$ nm) surrounding the mercury lamp, which removed shorter wavelength radiation that is not contained in the terrestrial solar spectrum. Visible light irradiation experiments used a 100-W halogen lamp (Phillips). All irradiated ice samples were thawed for sampling and the subsequent analysis of the dissolved Mn^{2+}. Aqueous photochemical reactions of colloidal manganese oxide were also carried out as a control at 25 °C using the same experimental setup. Dark dissolution experiments were carried out under the same experimental conditions except for the absence of light. All reactions were repeated at least two or three times to confirm the reproducibility.

Analysis. Five milliliter aliquots of the sample solution were withdrawn from the quartz reaction tube after thawing the ice sample. The liquid aliquot was filtered with 0.1 μm syringe filter

and then added to a vial containing 5 mL distilled water (to dilute Mn^{2+} for optimal analysis). The colloidal MnO_2 was successfully removed by the syringe filter as shown in Figure 1d. After filtration and dilution, the amount of dissolved Mn^{2+} was measured by atomic absorption spectrophotometer (Varian Spectra AA 800). The UV light intensity absorbed by aqueous and ice samples was compared by ferrioxalate actinometry.[28] The ferrioxalate solution was solidified prior to irradiation, irradiated under the same condition as the manganese oxide photolysis, and the photogenerated Fe^{2+} was analyzed after thawing in the dark. The UV intensity absorbed by the aqueous and ice samples was estimated to be 3.0×10^{-4} and 1.4×10^{-4} einstein min^{-1} L^{-1} ($\lambda > 300$ nm), respectively, even under the same irradiation condition. The lower absorbed intensity for the ice sample is ascribed to the light scattering loss by the turbid ice samples. The optical images of ice were obtained with a Zeiss JENALAB-pol polarizing microscope equipped with a Linkam LTS 350 thermal stage (temperature range of −196 to 350 °C) and a Linkam LNP94 liquid nitrogen pump. One or two droplets of sample solutions were dropped on the cover glass and put on the stage. The desired temperature (−20 °C) of the airtight stage containing sample solution was controlled by the liquid nitrogen pump. It took 2 min to cool the stage at −20 °C.

Outdoor Experiment. The photodissolution experiments were also carried out under ambient solar radiation. Since the freezing temperature is not attained and the solar flux is highly variable in our geographical location and season, the outdoor experiments were conducted in the arctic region, Ny-Ålesund (78°55′N, 11°56′E, sea level) from May 17 to 18, 2010 where the sunlight is available for 24 h a day. Quartz tubes containing the manganese oxide with electron donors were frozen in a refrigerator before exposing to sunlight. The solidified ice samples were placed on the surface of ambient snow horizontally for exposure to incident solar radiation. The irradiated samples remained solid during the entire exposure to sunlight. Control photolysis of aqueous samples containing manganese oxide was carried out simultaneously under the same irradiation condition. In order to prevent the freezing of the aqueous samples under outdoor condition, samples were placed on an electrically heated mat on the snow. The irradiated samples were directly filtered on site (DASAN Station, KOPRI) and stored and transported back to our laboratory for the quantification of photogenerated Mn^{2+}. The ambient temperature in the arctic location ranged between 0.9 and 2.3 °C. The integrated solar irradiance as measured at the Koldewey Station in Ny-Ålesund varied from 19.2 to 29.4 W/m^2 for the UV band of $300 < \lambda < 370$ nm, depending on the angular position of the sun and the weather condition with a daily average of 23 W/m^2 (corresponding to about 65 μEinstein $m^{-2}sec^{-1}$ assuming 335 nm photons).

■ RESULTS AND DISCUSSION

Reductive Dissolution of Manganese Oxide. The formation of Mn(II)$_{aq}$ via reductive dissolution of colloidal MnO_2 was investigated under both irradiation and dark conditions in the presence of several organic acids as an electron donor (ED). We found that the photoreductive dissolution of MnO_2 in ice under UV irradiation of $\lambda > 300$ nm was about 5 times higher than in aqueous solution despite the lower UV intensity absorbed by the ice sample (Figure 2a). The accelerated dissolution of MnO_2 in ice was observed even in the absence of UV irradiation (about 3 times enhanced compared
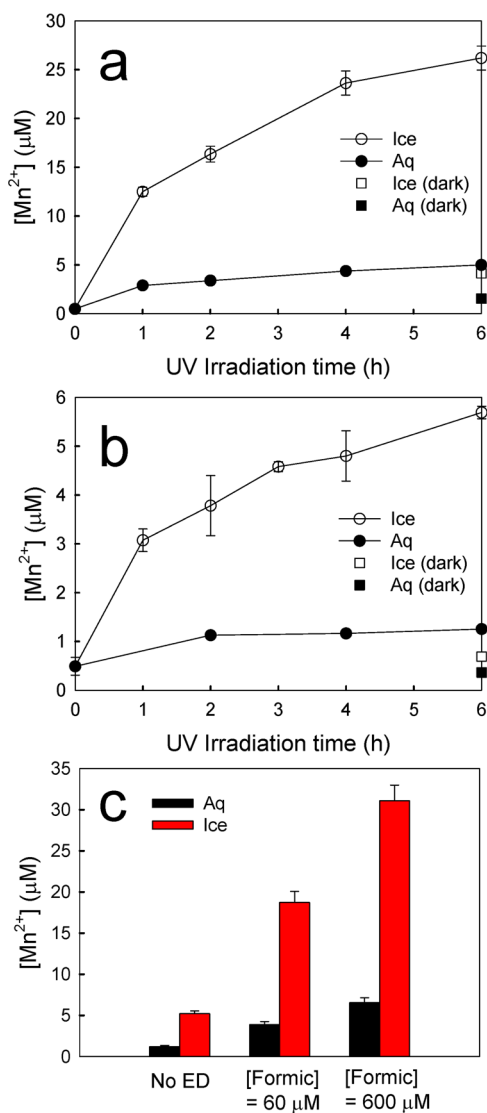
Figure 2. (a) Time profile of $Mn(II)_{aq}$ formation via photoreductive dissolution of birnessite under UV light ($\lambda > 300$ nm) in aqueous solution at 25 °C and ice at −20 °C. Dissolution in the dark condition is compared as well. Experimental conditions were as follows: $[MnO_2]$ = 4.35 mg/L (50 μM), [formic acid] = 600 μM, pH_i = 3.6 (no pH adjustment). (b) Similar time profile of photoreductive dissolution of birnessite under UV light ($\lambda > 300$ nm) in a different experimental condition: $[MnO_2]$ = 4.35 mg/L (50 μM), [formic acid] = 60 μM, pH_i = 5. (c) Comparison of the photoreductive dissolution of MnO_2 with different concentrations of formic acid as an electron donor in aqueous solution (black bar) and ice phase (red bar) at the same pH_i = 3.0. [Mn(II)] was measured after 6 h irradiation. Experimental conditions were as follows: $[MnO_2]$ = 4.35 mg/L (50 μM).

to that in liquid water) though the rate was much reduced compared with the photodissolution rate. In order to simulate more realistic condition, we carried out the MnO_2 dissolution experiment with lower concentrations of ED and proton (pH 5, acidity level found in polar snow and ice)[29,30] and the results are shown in Figure 2b. The enhanced photodissolution of MnO_2 was similarly observed. The concentration effect of ED (formic acid) on the photodissolution was compared at the same initial pH of 3 in Figure 2c. The ice-enhanced effect markedly increased with increasing the formic acid concentration. This confirms the critical role of ED in the photodissolution of MnO_2 in ice. It should be also noted that

the ice-enhanced dissolution of MnO_2 was observed even in the absence of organic ED. This implies that the ice-enhanced dissolution of MnO_2 should be also applicable to environmental conditions where the concentration of EDs is very low.

The formation of $Mn(II)_{aq}$ via photoreductive dissolution was investigated in the presence of various organic acids as an ED. As for the photodissolution, the ice-enhanced effect was observed with all EDs tested and particularly outstanding with formic and oxalic acid (Figure 3). In the presence of oxalic acid,
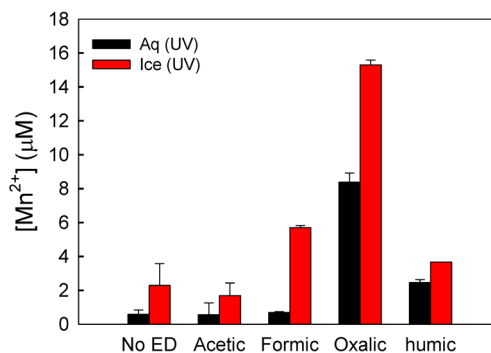

Figure 3. Comparison of $Mn(II)_{aq}$ generation in the presence of various organic acids as ED in aqueous solution at 25 °C and ice at −20 °C under UV irradiation (6 h). Experimental conditions were as follows: $[MnO_2]$ = 4.35 mg/L (50 μM), [ED] = 60 μM, [humic acid] = 1 ppm, pH_i = 5.

the dissolution of MnO_2 shows the highest rate both in aqueous and ice phase under UV light irradiation since oxalic acid forms strong surface complex on metal oxides.[6,27] The oxidation potentials for formic, acetic, and oxalic acid are 0.2, −0.074, and 0.63 V (vs NHE),[31,32] respectively, which also supports the highest efficiency of oxalic acid as an ED. It is noted that the reductive dissolution of MnO_2 in ice under UV irradiation was enhanced even in the absence of ED and the dissolution rate was gradually increased with increasing the added ED concentration. In our previous work,[13] we hypothesized that the electron hopping within the agglomerates of iron oxide particles trapped in ice grain boundaries may facilitate the charge-pair separation in the semiconductor lattice. The same explanation might be applied to this case of MnO_2 that is a semiconductor.

We also studied the pH effect on the reductive dissolution of MnO_2 both in the presence and absence of light (Figure 4). It was previously estimated that the local concentration of acids in the ice grain boundary region can be enhanced by 2−4 orders of magnitude in contrast to the aqueous solution using cresol red as a probe.[18] The pH of unfrozen solution in ice grain boundaries can be affected by not only the freeze concentration effect of acidic/basic substrates, but also the freeze potential effect (which is induced when the distribution of cations and anions during freezing is not uniform). For example, the preferential incorporation of cations (e.g., NH_4^+, Na^+) within the ice matrix makes OH^- immigrate onto ice surface to neutralize the positive ice potential, which leaves more protons in the unfrozen solution (more acidic).[18] Therefore, the electrolyte concentration and composition should be also taken into account when investigating the pH effect, which implies that the pH effect may be complex depending on the solution properties. The reductive dissolution gradually decreased with increasing pH in both cases. The ice-enhanced dissolution of MnO_2 in the dark was more marked at acidic pH
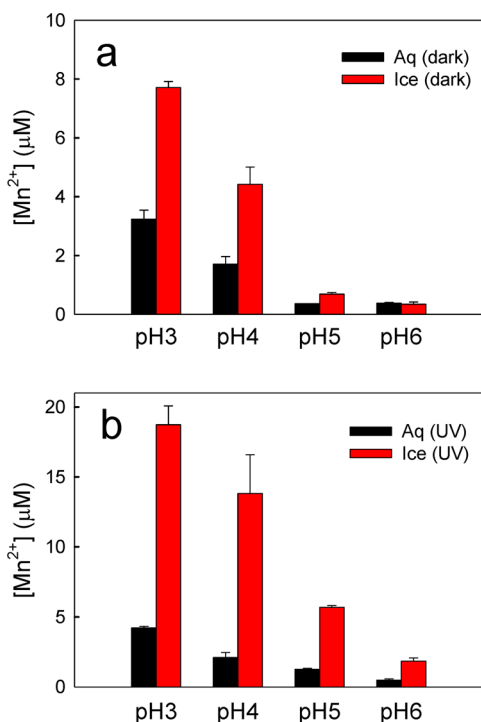
Figure 4. pH dependence of $Mn(II)_{aq}$ production in aqueous and ice phase. (a) $Mn(II)_{aq}$ formation in the absence of light. (b) $Mn(II)_{aq}$ formation under UV irradiation. Experimental conditions were as follows: $[MnO_2] = 4.35$ mg/L (50 μM), [formic acid] = 60 μM, 6 h reaction time.

and negligible above pH 6. The photoreductive dissolution of MnO_2 in ice phase exhibited a similar pH dependence and the ice-enhanced effect was observed up to pH 6.

The photoreductive dissolution experiments were also carried out under visible light illumination ($\lambda > 400$ nm) since most of solar photon energy is in the visible-spectrum region (Figure 5). Although the concentration of dissolved
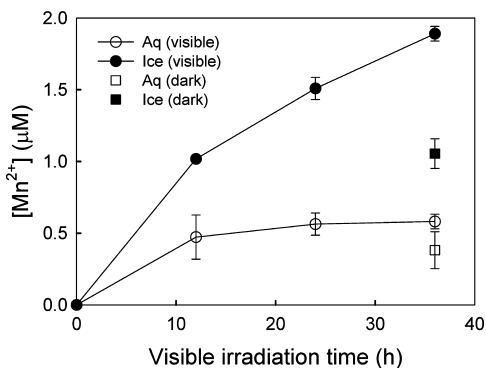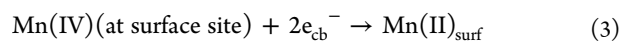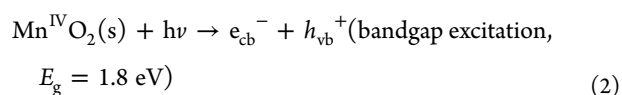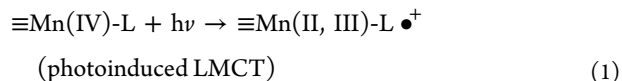

Figure 5. Photoreductive dissolution of MnO_2 colloid under visible light ($\lambda > 400$ nm, 100-W halogen lamp), $[MnO_2] = 4.35$ mg/L (50 μM), [formic acid] = 60 μM, $pH_i = 5$.

$Mn(II)_{aq}$ under visible light irradiation was smaller than under UV light, a similar trend was observed. The $Mn(II)_{aq}$ dissolution from colloidal MnO_2 was clearly enhanced in ice phase in both visible irradiation and dark conditions.

In order to verify that the results observed in the laboratory are viable under natural sunlight condition, the photoreductive dissolution experiment of MnO_2 was also carried out under the
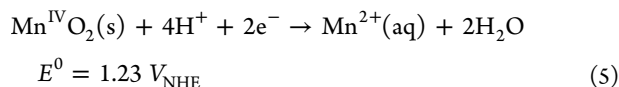
Arctic solar condition (Ny-Ålesund, Svalbard, 78°55′N). The concentration of Mn^{2+}_{aq} (generated under the condition of $[MnO_2] = 4.35$ mg/L, [formic acid] = 60 μM, pH = 4.6) after 4.5 h exposure to arctic sunlight was 3.1 and 6.7 μM in aqueous solution and ice, respectively. The photoreductive dissolution of MnO_2 under the Arctic solar irradiation was also enhanced (about 2-fold) in ice phase compared to the aqueous counterpart, which confirmed the laboratory observation (about 5-fold enhancement). The Arctic irradiation intensity (3.9×10^{-7} einstein min^{-1} cm^{-2}) was comparable to the laboratory one (3.0×10^{-7}) and the photodissolution rates of MnO_2 in ice under the Arctic and the laboratory conditions were also similar to be 19 and 14 μg Mn/(mg MnO_2)·h (at pH 4.6 and 5.0), respectively.

Reductive Dissolution Mechanism. The dissolution of MnO_2 is a reductive process and organic ligands complexed on the surface usually induce such process through ligand-to-metal charge transfer (LMCT) upon photoexcitation. The photo-reductive dissolution of MnO_2 via LMCT should consist of the following steps: (1) surface complexation between an organic reductant (or ligand, L) and the surface Mn(IV); (2) electron transfer from the organic ligand to Mn(IV) with generating an oxidized ligand and a reduced Mn(II)/Mn(III) species (eq 1); (3) desorption of reduced Mn(II) on the surface into the solution (eq 4). The electron transfer from organic ligands to surface Mn(IV) species is induced by photon absorption (i.e., photoinduced LMCT). An alternative mechanism of the photoreductive dissolution is based on the semiconductor model. The bandgap excitation of MnO_2 (semiconductor with $E_g = 1.8$ eV) generates charge pairs in the semiconductor lattice (eq 2) and the electron in the conduction band subsequently transfer to the surface Mn(IV) species to generate Mn(II) species (eq 3).[33] The bandgap excitation model should work only under irradiation while the reductive dissolution occurs under both irradiated and dark conditions.[33,34]
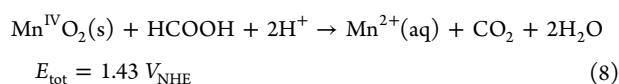
$$\equiv Mn(IV)\text{-}L + h\nu \rightarrow \equiv Mn(II, III)\text{-}L \bullet^+$$
$$(\text{photoinduced LMCT}) \tag{1}$$

$$Mn^{IV}O_2(s) + h\nu \rightarrow e_{cb}^- + h_{vb}^+ (\text{bandgap excitation,}$$
$$E_g = 1.8 \text{ eV}) \tag{2}$$

$$Mn(IV)(\text{at surface site}) + 2e_{cb}^- \rightarrow Mn(II)_{surf} \tag{3}$$

$$Mn(II)_{surf} \rightarrow Mn(II)_{aq} \tag{4}$$

It should be noted that the dark reductive dissolution of MnO_2 by formic acid in ice phase was 2−3 times enhanced than in aqueous matrices even in the absence of light (Figure 4a). According to the redox chemical equation (eqs 5, 6, 8), the reduction of MnO_2 by formic acid is thermodynamically spontaneous. Since the reductive dissolution of MnO_2 is favored at acidic condition (eq 8), the elevated concentration of protons and formic acids in the ice grain boundary seems to be responsible for the enhanced reductive dissolution in the dark. In our previous work, the formation of Fe^{2+}_{aq} from Fe_2O_3 via reductive dissolution in the presence of formic acid was negligible in the dark,[13] whereas the reductive dissolution of MnO_2 in this work was not insignificant. Although both dissolution reactions are thermochemically spontaneous (eq 8 vs eq 11), MnO_2 dissolution has a much higher driving force than the Fe_2O_3 dissolution. In addition, the dissolution in the
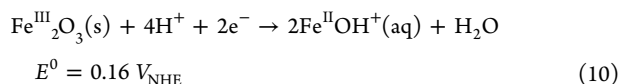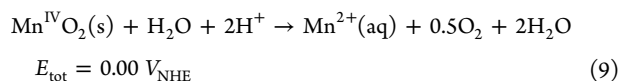
absence of organic EDs (where water should work as a reductant: eq 7) shows a similar trend (eq 9 vs eq 12): MnO_2 dissolution is weakly allowed, whereas the Fe_2O_3 dissolution is thermochemically nonspontaneous. Therefore, the dissolution of MnO_2 is more favored than that of Fe_2O_3 whether there is an organic reductant or not. This seems to be why the dissolution of MnO_2 is not negligible in the absence of either light or organic EDs in ice.
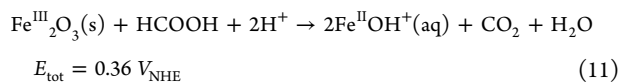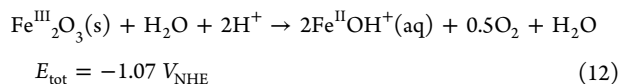
$$Mn^{IV}O_2(s) + 4H^+ + 2e^- \rightarrow Mn^{2+}(aq) + 2H_2O$$
$$E^0 = 1.23\ V_{NHE} \tag{5}$$

$$CO_2 + 2H^+ + 2e^- \rightarrow HCOOH\ E^0 = -0.196\ V_{NHE} \tag{6}$$

$$0.5O_2 + 2H^+ + 2e^- \rightarrow H_2O\ E^0 = 1.23\ V_{NHE} \tag{7}$$

Net reaction with formic acid:

$$Mn^{IV}O_2(s) + HCOOH + 2H^+ \rightarrow Mn^{2+}(aq) + CO_2 + 2H_2O$$
$$E_{tot} = 1.43\ V_{NHE} \tag{8}$$

Net reaction without organic electron donor:

$$Mn^{IV}O_2(s) + H_2O + 2H^+ \rightarrow Mn^{2+}(aq) + 0.5O_2 + 2H_2O$$
$$E_{tot} = 0.00\ V_{NHE} \tag{9}$$

$$Fe^{III}_2O_3(s) + 4H^+ + 2e^- \rightarrow 2Fe^{II}OH^+(aq) + H_2O$$
$$E^0 = 0.16\ V_{NHE} \tag{10}$$

Net reaction with formic acid:

$$Fe^{III}_2O_3(s) + HCOOH + 2H^+ \rightarrow 2Fe^{II}OH^+(aq) + CO_2 + H_2O$$
$$E_{tot} = 0.36\ V_{NHE} \tag{11}$$

Net reaction without organic electron donor:

$$Fe^{III}_2O_3(s) + H_2O + 2H^+ \rightarrow 2Fe^{II}OH^+(aq) + 0.5O_2 + H_2O$$
$$E_{tot} = -1.07\ V_{NHE} \tag{12}$$

The MnO_2 particles and the organic reductants can be highly concentrated in the liquid-like ice grain boundary region through freeze concentration effect. Under such conditions, the surface complexation between manganese oxide particles and organic ligands should be enhanced to accelerate the reductive dissolution. The highly aggregated manganese oxide particles within the ice grain boundaries were actually observed by optical microscopy as shown in Figure 1e. The chemical environments such as the concentration of solutes, ionic strength, and pH in liquid-like ice grain boundary are different from those in aqueous solution, which may create a unique reaction condition and be responsible for the ice-enhanced dissolution of MnO_2.[11−13,16,35] In addition, the electron and hole pair separation among MnO_2 agglomerates confined in the ice grain boundaries can be enhanced by the electron hopping through interlinked semiconductor nanoparticles and the following interfacial electron transfer processes can be also enhanced compared to those occurring on isolated nano-particles in the aqueous solution.[13,36,37]

Environmental Relevance. The primary finding from this study is that the formation of $Mn(II)_{aq}$ via (photo) reductive dissolution of MnO_2 can be enhanced by several times in ice phase compared to the aqueous dissolution reaction. Such effect was observed in both irradiated and dark condition although the ice-enhanced effect was more outstanding under the irradiation. Manganese can be found in a variety of environmental media such as soil, sediments, atmospheric water, freshwater, seawater, groundwater, and acid mine drainage. Manganese is the 12th most abundant element (about 0.1%) that constitutes the Earth's crust and soil typically contains manganese (average of 440 ppm).[38] Similarly, the manganese concentration in the liquid fraction of aerosol, cloud, fog, and rain ranges in 0.01−100 μM.[39] The manganese, like iron, is also an essential trace nutrient for all life on earth because of its role as enzyme cofactor and photosynthetic oxygen evolution. In order to be used for living organisms, the solid form of manganese oxide should be converted into soluble form of manganese (normally $Mn(II)_{aq}$). The present finding is of significant eco-environmental importance because it suggests a new pathway of bioavailable Mn species generation.

The environmental implications of this work are broad and various environmental media with the frozen state can be related with this phenomenon. The redox transformation of manganese significantly influences the speciation, solubility, mobility, toxicity, and bioavailability of various organic and inorganic species including arsenic, chromium, cobalt, and selenium.[2,3] Aeolian mineral dust particles containing MnO_2 can be trapped in cloud droplets in upper troposphere during atmospheric transportation and experience freeze−thaw cycles. This process should induce the production of more soluble form of manganese before deposition onto sea surface according to the ice-enhanced dissolution phenomenon observed in this work. Such an hypothesis is consistent with the previous reports that the soluble fraction of mineral increased from ∼1% to 10−40% in remote ocean region compared to that in the origin place.[40,41] In a similar way, manganese mineral trapped in sea ice could be transformed to a more soluble form and provide more bioavailable manganese to the ocean. Snow and ice containing manganese oxide may also contribute to the supply of more usable manganese ($Mn(II)_{aq}$) to marine phytoplankton, consequently affecting CO_2 uptake by stimulating a biological pump in the polar ocean.[9,42] The present observation that the manganese dissolution was enhanced in ice phase even in the absence of light also implies that Mn-containing soil may provide more bioavailable manganese into the soil environment when the frozen soil melts. However, more detailed investigations need to be done in order to find out the real environmental effects of the present laboratory results.

■ AUTHOR INFORMATION

Corresponding Author

*Fax: +82-54-279-8299; e-mail: wchoi@postech.edu.

Notes

The authors declare no competing financial interest.

■ REFERENCES

(1) Borch, T.; Kretzschmar, R.; Kappler, A.; Cappellen, P.; Ginder-Vogel, M.; Voegelin, A.; Cambell, K. Biogeochemical redox processes and their impact on contaminant dynamics. *Environ. Sci. Technol.* **2010**, *44*, 15−23.

(2) Manning, B. A.; Fendorf, S. T.; Bostick, B.; Suarez, D. L. Arsenic(III) oxidation and arsenic(V) adsorption reactions on synthetic birnessite. *Environ. Sci. Technol.* **2002**, *36*, 976−981.

(3) Post, J. E. Manganese oxide minerals: Crystal structures and economic and environmental significance. *Proc. Natl. Acad. U.S.A.* **1999**, *96*, 3447−3454.

(4) Stone, A. T.; Morgan, J. J. Reduction and dissolution of manganese(III) and manganese(IV) oxides by organics: 2. Survey of the reactivity of organics. *Environ. Sci. Technol.* **1984**, *18* (8), 617−624.

(5) Stone, A. T.; Morgan, J. J. Reduction and dissolution of manganese(III) and manganese(IV) oxides by organics: 1. Reaction with hydroquinone. *Environ. Sci. Technol.* **1984**, *18*, 450−456.

(6) Xyla, A. G.; Silzberger, B.; G., W. L., III; Hering, J. G.; Cappellen, P. V.; Stumm, W. Reductive dissolution of manganese(III,IV) (Hydr)oxides by oxalate: The effect of pH and light. *Langmuir* **1992**, *8*, 95−103.

(7) Waite, T. D.; Wrlgley, I. C.; Szymczak, R. Photoassisted dissolution of a colloidal manganese oxide in the presence of fulvic acid. *Environ. Sci. Technol.* **1988**, *22* (7), 778−785.

(8) Sunda, W. G.; Kieber, D. J. Oxidation of humic substances by manganese oxides yields low-molecular-weight organic substrates. *Nature* **1994**, *367*, 62−64.

(9) Sunda, W. G.; Huntsman, S. A.; Harvey, G. R. Photoreduction of manganese oxides in seawater and its geochemical and biological implication. *Nature* **1983**, *301*, 234−236.

(10) Finden, D. A. S.; Tipping, E.; Jaworski, G. H. M.; Reynolds, C. S. Light-induced reduction of natural iron(III) oxide and its relevance to phytoplankton. *Nature* **1984**, *309*, 783−784.

(11) Takenaka, N.; Ueda, A.; Daimon, T.; Bandow, H.; Dohmaru, T.; Maeda, Y. Acceleration mechanism of chemical reaction by freezing: the reaction of nitrous acid with dissolved oxygen. *J. Phys. Chem.* **1996**, *100*, 13874−13884.

(12) Takenaka, N.; Ueda, A.; Maeda, Y. Acceleration of the rate of nitrite oxidation by freezing in aqueous solution. *Nature* **1992**, *358*, 736−738.

(13) Kim, K.; Choi, W.; Hoffmann, M. R.; Yoon, H.-I.; Park, B.-K. Photoreductive dissolution of iron oxides trapped in ice and its environmental implications. *Environ. Sci. Technol.* **2010**, *44*, 4142−4148.

(14) Kim, K.; Choi, W. Enhanced redox conversion of chromate and arsenite in ice. *Environ. Sci. Technol.* **2011**, *45*, 2202−2208.

(15) Grannas, A. M.; Bausch, A. R.; Mahanna, K. M. Enhanced aqueous photochemical reaction rates after freezing. *J. Phys. Chem. A* **2007**, *111* (43), 11043−11049.

(16) Grannas, A. M.; Jones, A. E.; Dibb, J.; Ammann, M.; Anastasio, C.; Beine, H. J.; Bergin, M.; Bottenheim, J.; Boxe, C. S.; Carver, G.; Chen, G.; Crawford, J. H.; Dominé, F.; Frey, M. M.; Guzḿan, M. I.; Heard, D. E.; Helmig, D.; Hoffmann, M. R.; Honrath, R. E.; Huey, L. G.; Hutterli, M.; Jacobi, H. W.; Klán, P.; Lefer, B.; McConnell, J.; Plane, J.; Sander, R.; Savarino, J.; Shepson, P. B.; Simpson, W. R.; Sodeau, J. R.; Glasow, R. v.; Weller, R.; Wolff, E. W.; Zhu, T. An overview of snow photochemistry: Evidence, mechanisms and impacts. *Atmos. Chem. Phys.* **2007**, *7*, 4329−4373.

(17) Heger, D.; Jirkovsky, J.; Klan, P. Aggregation of methylene blue in frozen aqueous solutions studied by absorption spectroscopy. *J. Phys. Chem. A* **2005**, *109*, 6702−6709.

(18) Heger, D.; Klanova, J.; Klan, P. Enhanced protonation of Cresol red in acidic aqueous solutions caused by freezing. *J. Phys. Chem. B* **2006**, *110*, 1277−1287.

(19) Takenaka, N.; Bandow, H. Chemical kinetics of reactions in the unfrozen solution of ice. *J. Phys. Chem. A* **2007**, *111* (36), 8780−8786.

(20) Betterton, E. A.; Anderson, D. J. Autoxidation of N(III), S(IV), and other species in frozen solution—A possible pathway for enhanced chemical transformation in freezing systems. *J. Atmos. Chem.* **2001**, *40*, 171−189.

(21) Boxe, C. S.; Colussi, A. J.; Hoffmann, M. R.; Perez, I. M.; Murphy, J. G.; Cohen, R. C. Kinetics of NO and NO_2 evolution from illuminated frozen nitrate solutions. *J. Phys. Chem. A* **2006**, *110*, 3578−3583.

(22) Blaha, L.; Klanova, J.; Klan, P.; Janosek, J.; Skarek, M.; Ruzicka, R. Toxicity increases in ice containing monochlorophenols upon photolysis: Environmental consequences. *Environ. Sci. Technol.* **2004**, *38*, 2873−2878.

(23) Klanova, J.; Klan, P.; Nosek, J.; Holoubek, I. Environmental ice photochemistry: Monochlorophenols. *Environ. Sci. Technol.* **2003**, *37*, 1568−1574.

(24) Domine, F.; Shepson, P. B. Air−Snow interactions and atmospheric chemistry. *Science* **2002**, *297*, 1506−1510.

(25) Kahan, T. F.; Donaldson, D. J. Benzene photolysis on ice: Implications for the fate of organic contaminants in the winter. *Environ. Sci. Technol.* **2010**, *44* (10), 3819−3824.

(26) Perez-benito, J. F.; Arias, C.; Amat, E. A kinetic study of the reduction of colloidal manganese dioxide by oxalic acid. *J. Collid Interface Sci.* **1996**, *177*, 288−297.

(27) Banerjee, D.; Nesbitt, H. W. XPS study of reductive dissolution of birnessite by oxalate: Rates and mechanistic aspects of dissolution and redox processes. *Geochim. Cosmochim. Acta* **1999**, *63*, 3025−3038.

(28) Hatchard, C. G.; Parker, C. A. A new sensitive chemical actinometer. II. Potassium ferrioxalate as a standard chemical actinometer. *Proc. R. Soc. London, A* **1956**, *235*, 518−536.

(29) De Caritat, P.; Hall, G.; G slason, S.; Belsey, W.; Braun, M.; Goloubeva, N.; Olsen, H.; Scheie, J.; Vaive, J. Chemical composition of arctic snow: concentration levels and regional distribution of major elements. *Sci. Total Environ.* **2005**, *336*, 183−199.

(30) DeFelice, T. Chemical composition of fresh snowfalls at Palmer Station, Antarctica. *Atmos. Environ.* **1998**, *33*, 155−161.

(31) Zhang, X. V.; Ellery, S. P.; Friend, C. M.; Holland, H. D.; Michel, F. M.; Schoonen, M. A. A.; Martin, S. T. Photodriven reduction and oxidation reactions on colloidal semiconductor particles: Implications for prebiotic synthesis. *J. Photochem. Photobiol., A* **2007**, *185*, 301−311.

(32) Colucci, J.; Montalvo, V.; Hernandez, R.; Poullet, C. Electrochemical oxidation potential of photocatalyst reducing agents. *Electrochim. Acta* **1999**, *44*, 2507−2014.

(33) Sherman, D. M. Electronic structures of iron and manganese (hydr)oxide minerals_ Thermodynamics of photochemical reductive dissolution in auqatic environments. *Geochim. Cosmochim. Acta* **2005**, *69*, 3249−3255.

(34) Perez-benito, J. F.; Arias, C. A kinetic study of the reaction between soluble (colloidal) manganese dioxide and formic acid. *J. Colloid Interface Sci.* **1991**, *149*, 92−97.

(35) Cho, H.; Shepson, P. B.; Barrie, L. A.; Cowin, J. P.; Zaveri, R. *J. Phys. Chem. A* **2002**, *106*, 11226−11232.

(36) Wang, C.-y.; Pagel, R.; Dohrmann, J. K.; Bahnemann, D. W. Antenna mechanism and deaggregation concept: Novel mechanistic principles for photocatalysis. *C. R. Chim.* **2006**, *9*, 761−773.

(37) Lakshminarasimhan, N.; Kim, W.; Choi, W. Effect of the agglomerated state on the photocatalytic hydrogen production with In situ agglomeration of colloidal TiO_2 nanoparticles. *J. Phys. Chem. C* **2008**, *112* (51), 20451−20457.

(38) John, E. *Manganese, Nature's Building Blocks: An A-Z Guide to the Elements*; Oxford University Press: Oxford, 2001; pp 249−253.

(39) Seinfeld, J. H.; Pandis, S. N. *Atmospheric Chemistry and Physics: From Air Pollution to Climate Change*; John Wiley & Sons: Hoboken, NJ, 2006.

(40) Zhuang, G.; Yi, Z.; Duce, R. A.; Brown, P. R. Link between iron and sulphur cycles suggested by detection of ferrous in remote marine aerosols. *Nature* **1992**, *355*, 537−539.

(41) Fan, S.-M.; Moxim, W. J.; H. L., II Aeolian input of bioavailable iron to the ocean. *Geophys. Res. Lett.* **2006**, *33*, L07602.

(42) Chisholm, S. W. Stirring times in the Southern Ocean. *Nature* **2000**, *407*, 685−686.